Effective treatment of charge and spin fluctuations in dynamical and static atom-surface interactions

M. A. Romero,[1] F. Flores,[2] and E. C. Goldberg[1,3]

[1]*Instituto de Desarrollo Tecnológico para la Industria Química (INTEC), Consejo Nacional de Investigaciones Científicas y Técnicas (CONICET), Güemes 3450 CC 91, 3000 Santa Fe, Argentina*

[2]*Departamento Física Teórica de la Materia Condensada, Universidad Autónoma de Madrid, Madrid, Spain*

[3]*Departamento Ingeniería Materiales, Facultad de Ingeniería Química, Universidad Nacional del Litoral, Santiago del Estero 2829, 3000 Santa Fe, Argentina*

(Received 14 September 2009; revised manuscript received 16 November 2009; published 21 December 2009)

In this work we introduce a formalism that provides a good description of the correlated charge states of an atom interacting statically or dynamically with a metal surface, including realistic features of the atom-surface system. Our treatment of the Anderson impurity with an intrasite finite repulsion is based on the use of a projection operator technique and the application of the equation of motion method. The specific case of charge state configurations having zero, one, and two valence electrons of atoms with *s*-type valence orbital is discussed in this work. Static properties, such as the average occupation and the local density of states at the atom site and dynamical charge fractions in atom scattering processes, are compared with exact calculations and also with other existing approximations. Our treatment of the finite electronic repulsion at the atom site also reproduces satisfactorily the experimental behavior of the transmission phase shift of a dot measured by Aharonov-Bohm interferometry in both weak and strong coupling limits.

DOI: 10.1103/PhysRevB.80.235427 PACS number(s): 71.10.−w, 71.27.+a, 34.35.+a, 72.15.Qm

I. INTRODUCTION

To know the probability of the charge state configurations of atoms interacting with a surface is of great interest in many different physical situations such as chemisorption and ion scattering processes or quantum dots embedded in mesoscopic structures. The theoretical description of these systems is usually based on the Anderson model[1] in which the electronic correlations are confined to the single impurity atom or to the few impurities that represent the quantum dot. Several techniques have been developed to solve the impurity Anderson model,[2–20] but it still continues being an open problem with a rich variety of new proposals in the past years.[21–27] The renormalization group theory (RGT),[3,4] Bethe ansatz solution,[5–7] and quantum Monte Carlo technique[8,9] offer numerical exact calculations but limited to near equilibrium processes and to simplified descriptions of the interacting systems.

The effects of finite electron repulsion in a quantum dot can also be included by using perturbation theory in the correlation parameter, U.[17–19] Levy Yeyati *et al.* proposed an interesting extension of the second-order self-energy associated with the Coulomb interaction to high values of U.[20]

In the case of a finite but large electronic repulsion, equation of motion (EOM)[2,10–15,21–27] offers an easy way of handling realistic models for the atom-surface interacting system in and out of equilibrium,[28,29] and it is an appropriate method when time-dependent interactions are involved.[30,31] In the case of the single impurity Anderson model, the equation of motion of the single-particle Green's function gives rise to an infinite hierarchy of equations of motion for higher-order Green's functions. The level at which these higher-order Green's functions are truncated and the corresponding correlation functions are self-consistently determined marks the differences among the existing approximations.[10–15,21–27]

In this work we treat the case of atoms with an *s*-type valence orbital interacting with a surface and extend previous approaches[24,28] where an infinite U parameter has been assumed to the case of a finite U value. The atom can be an impurity, an adsorbate, or a projectile colliding with a surface; for a finite U the atom has four possible configuration states, with zero, one (spin up or down), and two electrons in the valence state. We describe the surface-atom interaction by projecting the Anderson Hamiltonian on the subspace of these atomic configurations and introduce the Green's functions required to calculate the magnitudes of interest such as the local density of states on the atom and the valence state occupation probabilities. These Green's functions are calculated using the EOM method and, at variance with other approaches, we truncate the set of higher-order Green's functions using a strict solution to order V^2,[24] V defining the order of magnitude of the coupling term between the atomic level and the band states, whereby the Green's functions containing off-diagonal terms in the band state index (see below) are neglected. It has been shown in Ref. 24 that this way of truncating the hierarchy of Green's functions provides a better solution to the EOM method. We present a description of the static and dynamic processes with the possibility of including in the calculation of the self-energies the main features of the electronic structure of the surface and the localized atom-atom interactions. In the case of an infinite value of the electronic intrasite repulsion U, this kind of formalism has proved to be successful for describing the charge exchange between a surface and the correlated states of an atom.[28–31] The finite U treatment presented in this work also allows us to reproduce the weak and strong coupling limits found in the transmission phase shift of a dot measured by Aharonov-Bohm interferometry.[32–35] The potentiality of this calculation for describing dynamical processes such as the collision between atoms and surfaces is tested in the simple

model of a many-body system consisting of an adatom attached to a substrate of three atoms. This model admits an exact solution of the Anderson-Newns Hamiltonian and has been already used for chemisorption studies[36,37] and also for testing approximations for the dynamical collision processes in the $U \to 0$ and $U \to \infty$ limit cases.[24,38]

II. THEORY

The starting point is the single impurity Anderson model[1] described by the following Hamiltonian:

$$\hat{H} = \sum_{\vec{k},\sigma} \varepsilon_{\vec{k}} \hat{n}_{\vec{k},\sigma} + \varepsilon_I \sum_{\sigma} \hat{n}_{a,\sigma} + \frac{U}{2} \sum_{\sigma} \hat{n}_{a,\sigma} \hat{n}_{a,\bar{\sigma}} + \sum_{\vec{k},\sigma} [V_{\vec{k},\sigma} \hat{c}^{\dagger}_{\vec{k},\sigma} \hat{c}_{a,\sigma} + \text{H.c.}], \quad (1)$$

where $\vec{k}$ denotes the solid states with energy $\varepsilon_{\vec{k}}$ and a denotes the "impurity" atom orbital state with energy ε_I. Their respective occupation number operators are $\hat{n}_{\vec{k},\sigma} = \hat{c}^{\dagger}_{\vec{k},\sigma} \hat{c}_{\vec{k},\sigma}$, $\hat{n}_{a,\sigma} = \hat{c}^{\dagger}_{a,\sigma} \hat{c}_{a,\sigma}$, σ being the spin projection index. The U parameter represents the intrasite electronic Coulomb repulsion in the unique considered atomic orbital a and $V_{\vec{k},\sigma}$ is the hopping integral between the solid and the impurity atom state. By assuming only one orbital state for the atom we are limiting its electronic configurations to zero, one (spins up and down), and two electrons in the same orbital. In such a case we are considering that other possible configurations (i.e., excited states of the impurity atom) have negligible probability of occurrence. An appropriate way of describing the possible atomic configurations within the Anderson description is by using a projection operator technique. Then, the electronic configurations of the atom are represented as follows: $|0,0\rangle$: zero electron, $|\uparrow,0\rangle$: one electron with "spin up," $|0,\downarrow\rangle$: one electron with "spin down," and $|\uparrow,\downarrow\rangle$: two electrons.

Taking into account this notation, the Hamiltonian that describes the impurity atom can be written as

$$H_{at} = E_0 |0,0\rangle\langle 0,0| + E_1 (|\uparrow,0\rangle\langle\uparrow,0| + |0,\downarrow\rangle\langle 0,\downarrow|) + E_2 |\uparrow,\downarrow\rangle\langle\uparrow,\downarrow|. \quad (2)$$

In Eq. (2) we have considered spin degeneration, and the total energies E_i are related to ε_I and U parameters of Eq. (1) in the following way:

$$E_1 - E_0 = \varepsilon_I,$$

$$E_2 - E_0 = 2\varepsilon_I + U = \varepsilon_A. \quad (3)$$

The correct normalization of the subspace including all the atomic configurations is the following:

$$|0,0\rangle\langle 0,0| + |\uparrow,0\rangle\langle\uparrow,0| + |0,\downarrow\rangle\langle 0,\downarrow| + |\uparrow,\downarrow\rangle\langle\uparrow,\downarrow| = \hat{1}. \quad (4)$$

We also have to write down the interaction Hamiltonian within the spirit of the Anderson model which involves only one-electron atom-solid interaction terms. The one to zero electron transition in the atom state corresponds to

$$\sum_{\vec{k}} V_{\vec{k},\uparrow} \hat{c}^{\dagger}_{\vec{k},\uparrow} \hat{c}_{a,\uparrow} |\uparrow,0\rangle = \sum_{\vec{k}} V_{\vec{k},\uparrow} \hat{c}^{\dagger}_{\vec{k},\uparrow} |0,0\rangle,$$

which implies that

$$\sum_{\vec{k}} V_{\vec{k},\uparrow} \hat{c}^{\dagger}_{\vec{k},\uparrow} \hat{c}_{a,\uparrow} \equiv \sum_{\vec{k}} V_{\vec{k},\uparrow} \hat{c}^{\dagger}_{\vec{k},\uparrow} |0,0\rangle\langle\uparrow,0|.$$

The same is valid in the case of a spin-down one-electron configuration. For transitions between one and two electrons in the atom,

$$\sum_{\vec{k}} V_{\vec{k},\uparrow} \hat{c}^{\dagger}_{\vec{k},\uparrow} \hat{c}_{a,\uparrow} |\uparrow,\downarrow\rangle = \sum_{\vec{k}} V_{\vec{k},\uparrow} \hat{c}^{\dagger}_{\vec{k},\uparrow} |0,\downarrow\rangle,$$

$$\sum_{\vec{k}} V_{\vec{k},\downarrow} \hat{c}^{\dagger}_{\vec{k},\downarrow} \hat{c}_{a,\downarrow} |\uparrow,\downarrow\rangle = -\sum_{\vec{k}} V_{\vec{k},\downarrow} \hat{c}^{\dagger}_{\vec{k},\downarrow} |\uparrow,0\rangle,$$

yielding

$$\sum_{\vec{k}} V_{\vec{k},\uparrow} \hat{c}^{\dagger}_{\vec{k},\uparrow} \hat{c}_{a,\uparrow} \equiv \sum_{\vec{k}} V_{\vec{k},\uparrow} \hat{c}^{\dagger}_{\vec{k},\uparrow} |0,\downarrow\rangle\langle\uparrow,\downarrow|,$$

$$\sum_{\vec{k}} V_{\vec{k},\downarrow} \hat{c}^{\dagger}_{\vec{k},\downarrow} \hat{c}_{a,\downarrow} \equiv -\sum_{\vec{k}} V_{\vec{k},\downarrow} \hat{c}^{\dagger}_{\vec{k},\downarrow} |\uparrow,0\rangle\langle\uparrow,\downarrow|$$

(notice the negative sign in the second equation). In this picture Anderson Hamiltonian (1) adopts the expression

$$\hat{H} = \sum_{\vec{k},\sigma} \varepsilon_{\vec{k}} \hat{n}_{\vec{k},\sigma} + E_0 |0\rangle\langle 0| + E_1 \sum_{\sigma} |\sigma\rangle\langle\sigma| + E_2 |\uparrow,\downarrow\rangle\langle\uparrow,\downarrow| + \sum_{\vec{k},\sigma} [V_{\vec{k},\sigma} \hat{c}^{\dagger}_{\vec{k},\sigma} |0\rangle\langle\sigma| + V^{*}_{\vec{k},\sigma} |\sigma\rangle\langle 0| \hat{c}_{\vec{k},\sigma}] + \sum_{\vec{k},\sigma} (-1)^{p_\sigma} [V_{\vec{k},\sigma} \hat{c}^{\dagger}_{\vec{k},\sigma} |\bar{\sigma}\rangle\langle\uparrow,\downarrow| + V^{*}_{\vec{k},\sigma} |\uparrow,\downarrow\rangle\langle\bar{\sigma}| \hat{c}_{\vec{k},\sigma}], \quad (5)$$

where we have introduced the following notation:

$$|\uparrow,0\rangle; |0,\downarrow\rangle \equiv |\sigma\rangle, \quad |0,0\rangle \equiv |0\rangle, \quad p_\sigma = \begin{cases} 0 & \text{if } \sigma = \uparrow \\ 1 & \text{if } \sigma = \downarrow. \end{cases}$$

Equation (5) defines our basic Hamiltonian. We can calculate the probabilities of the selected atomic configurations by means of the following advanced Green's functions in the static case and for equilibrium processes:

$$G_\sigma(t,t') = i\theta(t'-t) \langle \{ |\sigma\rangle\langle 0|_{t'}, |0\rangle\langle\sigma|_t \} \rangle, \quad (6)$$

$$G^{\sigma}_{\uparrow\downarrow}(t,t') = i\theta(t'-t) \langle \{ |\uparrow,\downarrow\rangle\langle\sigma|_{t'}, |\sigma\rangle\langle\uparrow,\downarrow|_t \} \rangle, \quad (7)$$

while for time-dependent or nonequilibrium stationary processes we require also to calculate these other Green-Keldysh functions,[40]

$$F_\sigma(t,t') = i\langle [|\sigma\rangle\langle 0|_{t'}, |0\rangle\langle\sigma|_t] \rangle, \quad (8)$$

$$F^{\sigma}_{\uparrow\downarrow}(t,t') = i\langle [|\uparrow,\downarrow\rangle\langle\sigma|_{t'}, |\sigma\rangle\langle\uparrow,\downarrow|_t] \rangle. \quad (9)$$

The [ ] and { } symbols indicate commutator and anticommutator, respectively, and $\langle\ \rangle$ means the average over the Heisenberg state Φ_0 that describes the interacting system. Hereafter, the possibility of a difference between the spin

projection values due to magnetic surfaces is kept. The Green's functions [Eqs. (6)–(9)] are calculated using the EOM method accordingly to Hamiltonian (5).

A. EOM method

The equation of motion of the Green's function [Eq. (6)] yields

$$i\frac{dG_\sigma(t,t')}{dt} = \delta(t'-t)\langle|\sigma\rangle\langle\sigma| + |0\rangle\langle 0|\rangle + \varepsilon_I G_\sigma(t,t') + \sum_{\vec{k}} V^*_{\vec{k},\sigma} G_\sigma(|0\rangle\langle 0|\hat{c}_{\vec{k},\sigma}) + \sum_{\vec{k},\sigma'} V^*_{\vec{k},\sigma'} G_\sigma(|\sigma'\rangle \times\langle\sigma|\hat{c}_{\vec{k},\sigma'}) - (-1)^{p_{\bar\sigma}}\sum_{\vec{k}} V_{\vec{k},\bar\sigma} G_\sigma(|0\rangle\langle\uparrow,\downarrow|\hat{c}^\dagger_{\vec{k},\bar\sigma}). \tag{10}$$

One needs now the equations of motion of the higher-order Green's functions defined as

$$G_A(|B\rangle\langle C|\hat{c}_{\vec{k},\sigma}) = i\theta(t'-t)\langle\{A(t'),|B\rangle\langle C|\hat{c}_{\vec{k},\sigma}(t)\}\rangle.$$

This leads to an infinite hierarchy of equations of motion that we have closed using a strict solution to order $V^2_{\vec{k}}$ like the following ones:

$$i\theta(t'-t)\langle\{|\sigma\rangle\langle 0|_{t'};|0\rangle\langle\sigma|\hat{c}^\dagger_{\vec{k}',\sigma'}\hat{c}_{\vec{k},\sigma'}(t)\}\rangle = G_\sigma(t,t')\langle\hat{c}^\dagger_{\vec{k}',\sigma'}\hat{c}_{\vec{k},\sigma'}\rangle^0,$$

$$i\theta(t'-t)\langle\{|\sigma\rangle\langle 0|_{t'};|\sigma'\rangle\langle\uparrow,\downarrow|\hat{c}_{\vec{k}',\sigma'}\hat{c}^\dagger_{\vec{k},\bar\sigma}(t)\}\rangle = G_\sigma(|\sigma'\rangle\langle\uparrow,\downarrow|)\langle\hat{c}_{\vec{k}',\sigma'}\hat{c}^\dagger_{\vec{k},\bar\sigma}\rangle^0\delta_{\bar\sigma,\sigma'},$$

$$i\theta(t'-t)\langle\{|\sigma\rangle\langle 0|_{t'};|\sigma'\rangle\langle 0|\hat{c}_{\vec{k}',\sigma'}\hat{c}_{\vec{k},\sigma}(t)\}\rangle = 0, \tag{11}$$

where the supra zero index indicates the average over the noninteracting system. Therefore, $\langle\hat{c}^\dagger_{\vec{k},\sigma}\hat{c}_{\vec{k}',\sigma}\rangle^0 = \langle\hat{n}_{\vec{k},\sigma}\rangle\delta_{\vec{k},\vec{k}'}$ is the Fermi distribution for a temperature T in the case of a metallic surface, $\langle\hat{n}_{\vec{k},\sigma}\rangle = f_{<\sigma}(\varepsilon_{\vec{k}}) = 1/(1+e^{(\varepsilon_{\vec{k},\sigma}-\mu)/k_BT})$, μ being the Fermi energy.

In this way we arrive to the following final equations for the required Green's functions (the details are given in Appendix):

$$i\frac{dG_\sigma(t,t')}{dt} = \delta(t'-t)\langle 1-\hat{n}_{a,\bar\sigma}\rangle_{t'} + \varepsilon_I G_\sigma(t,t') - i\theta(t'-t)\sum_{\vec{k}} D^{\bar\sigma}_{1\vec{k}}(t,t') + \int_{-\infty}^{\infty} d\tau[\Xi^A_{0\sigma} + \Xi^A_{<\bar\sigma}] \times G_\sigma + (-1)^{p_{\bar\sigma}}\int_{-\infty}^{\infty} d\tau[\Xi^A_{1\bar\sigma} - \Xi^A_{<\bar\sigma}]G^c_\sigma, \tag{12}$$

$$i\frac{dG^\sigma_{\uparrow\downarrow}(t,t')}{dt} = \delta(t'-t)\langle\hat{n}_{a,\sigma}\rangle_{t'} + (\varepsilon_A-\varepsilon_I)G^\sigma_{\uparrow\downarrow}(t,t') + i\theta(t'-t)\sum_{\vec{k}} D^\sigma_{2\vec{k}}(t,t') + \int_{-\infty}^{\infty} d\tau[\Xi^A_{0\bar\sigma} + \Xi^A_{1\sigma} - \Xi^A_{<\sigma}]G^\sigma_{\uparrow\downarrow} + (-1)^{p_\sigma}\int_{-\infty}^{\infty} d\tau\Xi^A_{<\sigma}G^{\sigma c}_{\uparrow\downarrow}, \tag{13}$$

$$i\frac{dF_\sigma(t,t')}{dt} = \varepsilon_I F_\sigma(t,t') - i\theta(t'-t_0)\sum_{\vec{k}}[2\langle\hat{n}_{\vec{k},\bar\sigma}\rangle - 1]D^{\bar\sigma}_{1\vec{k}}(t,t') + \int_{-\infty}^{\infty} d\tau[\Xi^R_{0\sigma} + \Xi^R_{<\bar\sigma}]F_\sigma + (-1)^{p_{\bar\sigma}}\int_{-\infty}^{\infty} d\tau[\Xi^R_{1\bar\sigma} - \Xi^R_{<\bar\sigma}]F^c_\sigma + \int_{-\infty}^{\infty} d\tau[\Omega_{0\sigma} + \Omega_{<\bar\sigma}]G_\sigma + (-1)^{p_{\bar\sigma}}\int_{-\infty}^{\infty} d\tau[\Omega_{1\bar\sigma} - \Omega_{<\bar\sigma}]G^c_\sigma, \tag{14}$$

$$i\frac{dF^\sigma_{\uparrow\downarrow}(t,t')}{dt} = (\varepsilon_A-\varepsilon_I)F^\sigma_{\uparrow\downarrow}(t,t') + i\theta(t'-t_0)\sum_{\vec{k}}[2\langle\hat{n}_{\vec{k},\sigma}\rangle - 1]D^\sigma_{2\vec{k}}(t,t') + \int_{-\infty}^{\infty} d\tau[\Xi^R_{0\bar\sigma} + \Xi^R_{1\sigma} - \Xi^R_{<\sigma}]F^\sigma_{\uparrow\downarrow} + (-1)^{p_\sigma}\int_{-\infty}^{\infty} d\tau\Xi^R_{<\sigma}F^{\sigma c}_{\uparrow\downarrow} + \int_{-\infty}^{\infty} d\tau[\Omega_{0\bar\sigma} + \Omega_{1\sigma} - \Omega_{<\sigma}]G^\sigma_{\uparrow\downarrow} + (-1)^{p_\sigma}\int_{-\infty}^{\infty} d\tau\Omega_{<\sigma}G^{\sigma c}_{\uparrow\downarrow}. \tag{15}$$

The new *crossed* Green's functions appearing in Eqs. (12)–(15) are defined as

$$G^c_\sigma(t,t') = i\theta(t'-t)\langle\{|\sigma\rangle\langle 0|_{t'},|\bar\sigma\rangle\langle\uparrow,\downarrow|_t\}\rangle,$$

$$F^c_\sigma(t,t') = i\langle[|\sigma\rangle\langle 0|_{t'},|\bar\sigma\rangle\langle\uparrow,\downarrow|_t]\rangle,$$

$$G^{\sigma c}_{\uparrow\downarrow}(t,t') = i\theta(t'-t)\langle\{|\uparrow,\downarrow\rangle\langle\sigma|_{t'},|0\rangle\langle\bar\sigma|_t\}\rangle,$$

$$F^{\sigma c}_{\uparrow\downarrow}(t,t') = i\langle[|\uparrow,\downarrow\rangle\langle\sigma|_{t'},|0\rangle\langle\bar\sigma|_t]\rangle, \tag{16}$$

and their equations of motion are given in Appendix.

The following quantities have been introduced in Eqs. (12)–(15),

$$D^{\sigma}_{1\vec{k}}(t,t') = V^{*}_{\vec{k},\sigma}(t)\langle|\sigma\rangle\langle 0|\hat{c}_{\vec{k},\sigma}\rangle_{t'} e^{i\varepsilon_{\vec{k}}(t'-t)}$$
$$+ (-1)^{p_{\bar{\sigma}}} V_{k,\sigma}(t)\langle|\uparrow,\downarrow\rangle\langle\bar{\sigma}|\hat{c}_{\vec{k},\sigma}\rangle^{*}_{t'} e^{-i(\varepsilon_{\vec{k}}-\varepsilon_A)(t'-t)},$$

$$D^{\sigma}_{2\vec{k}}(t,t') = -V_{\vec{k},\sigma}(t)\langle|\sigma\rangle\langle 0|\hat{c}_{\vec{k},\sigma}\rangle^{*}_{t'} e^{-i(\varepsilon_{\vec{k}}-\varepsilon_A)(t'-t)}$$
$$+ (-1)^{p_{\sigma}} V^{*}_{\vec{k},\sigma}(t)\langle|\uparrow,\downarrow\rangle\langle\bar{\sigma}|\hat{c}_{\vec{k},\sigma}\rangle_{t'} e^{i\varepsilon_{\vec{k}}(t'-t)}, \quad (17)$$

and also the time-dependent self-energies,

$$\Xi^{A}_{0\sigma}(t,\tau) = i\theta(\tau-t)\sum_{\vec{k}} \xi_{\vec{k},\sigma}(t,\tau),$$

$$\Xi^{A}_{1\sigma}(t,\tau) = i\theta(\tau-t)\sum_{\vec{k}} [\xi_{\vec{k},\sigma}(t,\tau) + \xi^{*}_{\vec{k},\sigma}(t,\tau)e^{-i\varepsilon_A(t-\tau)}],$$

$$\Xi^{A}_{<\sigma}(t,\tau) = i\theta(\tau-t)\sum_{\vec{k}} \langle\hat{n}_{\vec{k},\sigma}\rangle[\xi_{\vec{k},\sigma}(t,\tau) + \xi^{*}_{\vec{k},\sigma}(t,\tau)e^{-i\varepsilon_A(t-\tau)}], \quad (18)$$

which verify $\Xi^{R}(t,\tau) = [\Xi^{A}(\tau,t)]^{*}$.

The expressions of the Ω-like self-energies appearing in the differential equations of the F-Green's functions are given by

$$\Omega_{0\sigma}(t,\tau) = i\sum_{\vec{k}} [2\langle\hat{n}_{\vec{k},\sigma}\rangle - 1]\xi_{\vec{k},\sigma}(t,\tau),$$

$$\Omega_{1\sigma}(t,\tau) = i\sum_{\vec{k}} [2\langle\hat{n}_{\vec{k},\sigma}\rangle - 1][\xi_{\vec{k},\sigma}(t,\tau) + \xi^{*}_{\vec{k},\sigma}(t,\tau)e^{-i\varepsilon_A(t-\tau)}],$$

$$\Omega_{<\sigma}(t,\tau) = i\sum_{\vec{k}} [2\langle\hat{n}_{\vec{k},\sigma}\rangle - 1]\langle\hat{n}_{\vec{k},\sigma}\rangle[\xi_{\vec{k},\sigma}(t,\tau)$$
$$+ \xi^{*}_{\vec{k},\sigma}(t,\tau)e^{-i\varepsilon_A(t-\tau)}], \quad (19)$$

with $\xi_{\vec{k},\sigma}(t,\tau) = V^{*}_{\vec{k},\sigma}(t)V_{\vec{k},\sigma}(\tau)e^{-i\varepsilon_{\vec{k}}(t-\tau)}$.

1. Time-dependent Hamiltonian parameters: Dynamical processes

In this case we are mainly interested in calculating the probabilities of the different atomic charge configurations, $n_0(t) \equiv \langle|0\rangle\langle 0|\rangle_t$: probability of having zero electron, $n_{1\sigma}(t) \equiv \langle|\sigma\rangle\langle\sigma|\rangle_t$: probability of having one electron with spin projection σ, and $n_2(t) \equiv \langle|\uparrow,\downarrow\rangle\langle\uparrow,\downarrow|\rangle_t$: probability of having two electrons.

These charge state probabilities are obtained from their time derivatives given by the following expressions:

$$\frac{dn_{1\sigma}}{dt} = 2\,\mathrm{Im}\sum_{\vec{k}} [V^{*}_{\vec{k},\sigma}\langle|\sigma\rangle\langle 0|\hat{c}_{\vec{k},\sigma}\rangle_t - (-1)^{p_{\bar{\sigma}}}V^{*}_{\vec{k},\bar{\sigma}}\langle|\uparrow,\downarrow\rangle\langle\sigma|\hat{c}_{\vec{k},\bar{\sigma}}\rangle_t],$$

$$\frac{dn_2}{dt} = 2\,\mathrm{Im}\sum_{\vec{k}} [V^{*}_{\vec{k},\uparrow}\langle|\uparrow,\downarrow\rangle\langle 0,\downarrow|\hat{c}_{\vec{k},\uparrow}\rangle_t - V^{*}_{\vec{k},\downarrow}\langle|\uparrow,\downarrow\rangle\langle\uparrow,0|\hat{c}_{\vec{k},\downarrow}\rangle_t]. \quad (20)$$

Hence we need to calculate the correlation functions, $\langle|\sigma\rangle\langle 0|\hat{c}_{\vec{k},\sigma}\rangle_t$ and $\langle|\uparrow,\downarrow\rangle\langle\sigma|\hat{c}_{\vec{k},\bar{\sigma}}\rangle_t$. They are obtained from these F-Green's functions at equal time values,

$$F_{\sigma}(\hat{c}_{\vec{k},\sigma}) = i\langle[|\sigma\rangle\langle 0|_{t'};\hat{c}_{\vec{k},\sigma}(t')]\rangle = 2i\langle|\sigma\rangle\langle 0|\hat{c}_{\vec{k},\sigma}\rangle_{t'},$$

$$F^{\sigma}_{\uparrow\downarrow}(\hat{c}_{\vec{k},\bar{\sigma}}) = i\langle[|\uparrow,\downarrow\rangle\langle\sigma|_{t'};\hat{c}_{\vec{k},\bar{\sigma}}(t')]\rangle = 2i\langle|\uparrow,\downarrow\rangle\langle\sigma|\hat{c}_{\vec{k},\bar{\sigma}}\rangle_{t'}. \quad (21)$$

In particular, by integrating the equations of motion for $F_{\sigma}(\hat{c}_{\vec{k},\sigma})$ and $F^{\sigma}_{\uparrow\downarrow}(\hat{c}_{\vec{k},\bar{\sigma}})$ yields

$$F_{\sigma}(\hat{c}_{\vec{k},\sigma}) = -i\int_{t_0}^{t'} d\tau V_{\vec{k},\sigma}(\tau)\{F_{\sigma} + (-1)^{p_{\sigma}}F^{c}_{\sigma} - [2\langle\hat{n}_{\vec{k},\sigma}\rangle - 1]$$
$$\times[G_{\sigma} + (-1)^{p_{\sigma}}G^{c}_{\sigma}]\}e^{-i\varepsilon_{\vec{k}}(t'-\tau)},$$

$$F^{\sigma}_{\uparrow\downarrow}(\hat{c}_{\vec{k},\bar{\sigma}}) = -i\int_{t_0}^{t'} d\tau V_{\vec{k},\bar{\sigma}}(\tau)\{F^{\sigma c}_{\uparrow\downarrow} + (-1)^{p_{\bar{\sigma}}}F^{\sigma}_{\uparrow\downarrow} - [2\langle\hat{n}_{\vec{k},\bar{\sigma}}\rangle - 1]$$
$$\times[G^{\sigma c}_{\uparrow\downarrow} + (-1)^{p_{\bar{\sigma}}}G^{\sigma}_{\uparrow\downarrow}]\}e^{-i\varepsilon_{\vec{k}}(t'-\tau)}, \quad (22)$$

which require to know for their calculation the Green's functions [Eqs. (6)–(9) and (16)]. Details about the calculation procedure are given in Appendix.

2. Time-independent Hamiltonian parameters: Equilibrium processes

In the static case the following expressions are obtained by Fourier transforming Eqs. (12) and (13):

$$G_{\sigma}(\omega) = \frac{\langle|\sigma\rangle\langle\sigma| + |0\rangle\langle 0|\rangle - \sum_{\vec{k}} V^{*}_{\vec{k},\bar{\sigma}}\dfrac{\langle|\bar{\sigma}\rangle\langle 0|\hat{c}_{\vec{k},\bar{\sigma}}\rangle}{\tilde{\omega}-\varepsilon_{\vec{k}}} - (-1)^{p_{\bar{\sigma}}}\sum_{\vec{k}} V_{\vec{k},\bar{\sigma}}\dfrac{\langle|\sigma\rangle\langle\uparrow,\downarrow|\hat{c}^{\dagger}_{\vec{k},\bar{\sigma}}\rangle}{\tilde{\omega}+\varepsilon_{\vec{k}}-\varepsilon_A}}{\tilde{\omega}-\varepsilon_I-\Xi_{0\sigma}(\omega)-\Xi_{<\bar{\sigma}}(\omega)} + (-1)^{p_{\bar{\sigma}}}\frac{[\Xi_{1\bar{\sigma}}(\omega)-\Xi_{<\bar{\sigma}}(\omega)]}{\tilde{\omega}-\varepsilon_I-\Xi_{0\sigma}(\omega)-\Xi_{<\bar{\sigma}}(\omega)}G^{c}_{\sigma}(\omega), \quad (23)$$

$$G^{\sigma}_{\uparrow\downarrow}(\omega)=\frac{\langle|\uparrow,\downarrow\rangle\langle\uparrow,\downarrow|+|\sigma\rangle\langle\sigma|\rangle-\sum_{\vec{k}}V_{\vec{k},\sigma}\frac{\langle\hat{c}^{\dagger}_{\vec{k},\sigma}|0\rangle\langle\sigma|\rangle}{\tilde{\omega}+\varepsilon_{\vec{k}}-\varepsilon_A}+(-1)^{p_\sigma}\sum_{\vec{k}}V^{*}_{\vec{k},\sigma}\frac{\langle|\uparrow,\downarrow\rangle\langle\bar{\sigma}|\hat{c}_{\vec{k},\sigma}\rangle}{\tilde{\omega}-\varepsilon_{\vec{k}}}}{\tilde{\omega}+\varepsilon_I-\varepsilon_A-\Xi_{0\bar{\sigma}}(\omega)-[\Xi_{1\sigma}(\omega)-\Xi_{<\sigma}(\omega)]}$$
$$+(-1)^{p_\sigma}\frac{\Xi_{<\sigma}(\omega)}{\tilde{\omega}+\varepsilon_I-\varepsilon_A-\Xi_{0\bar{\sigma}}(\omega)-[\Xi_{1\sigma}(\omega)-\Xi_{<\sigma}(\omega)]}G^{\sigma c}_{\uparrow\downarrow}(\omega). \tag{24}$$

The crossed-Green's functions $G^{c}_{\sigma}(\omega)$ and $G^{\sigma c}_{\uparrow\downarrow}(\omega)$ obtained from Eqs. (A1) and (A2) are

$$G^{c}_{\sigma}(\omega)=\frac{-\sum_{\vec{k}}V_{\vec{k},\bar{\sigma}}\frac{\langle|\sigma\rangle\langle\uparrow,\downarrow|\hat{c}^{\dagger}_{\vec{k},\bar{\sigma}}\rangle}{\tilde{\omega}+\varepsilon_{\vec{k}}-\varepsilon_A}-(-1)^{p_{\bar{\sigma}}}\sum_{\vec{k}}V^{*}_{\vec{k},\bar{\sigma}}\frac{\langle|\bar{\sigma}\rangle\langle 0|\hat{c}_{\vec{k},\bar{\sigma}}\rangle}{\tilde{\omega}-\varepsilon_{\vec{k}}}}{\tilde{\omega}+\varepsilon_I-\varepsilon_A-\Xi_{0\sigma}(\omega)-[\Xi_{1\bar{\sigma}}(\omega)-\Xi_{<\bar{\sigma}}(\omega)]}+(-1)^{p_{\bar{\sigma}}}\frac{\Xi_{<\bar{\sigma}}(\omega)}{\tilde{\omega}+\varepsilon_I-\varepsilon_A-\Xi_{0\sigma}(\omega)-[\Xi_{1\bar{\sigma}}(\omega)-\Xi_{<\bar{\sigma}}(\omega)]}G_{\sigma}(\omega), \tag{25}$$

$$G^{\sigma c}_{\uparrow\downarrow}(\omega)=\frac{\sum_{\vec{k}}V^{*}_{\vec{k},\sigma}\frac{\langle|\uparrow,\downarrow\rangle\langle\bar{\sigma}|\hat{c}_{\vec{k},\sigma}\rangle}{\tilde{\omega}-\varepsilon_{\vec{k}}}+(-1)^{p_\sigma}\sum_{\vec{k}}V_{\vec{k},\sigma}\frac{\langle|0\rangle\langle\sigma|\hat{c}^{\dagger}_{\vec{k},\sigma}\rangle}{\tilde{\omega}+\varepsilon_{\vec{k}}-\varepsilon_A}}{\tilde{\omega}-\varepsilon_I-\Xi_{0\bar{\sigma}}(\omega)-\Xi_{<\sigma}(\omega)}+(-1)^{p_\sigma}\frac{[\Xi_{1\sigma}(\omega)-\Xi_{<\sigma}(\omega)]}{\tilde{\omega}-\varepsilon_I-\Xi_{0\bar{\sigma}}(\omega)-\Xi_{<\sigma}(\omega)}G^{\sigma}_{\uparrow\downarrow}(\omega). \tag{26}$$

The introduced self-energies are the Fourier transform of Eq. (18), $(\tilde{\omega}=\omega-i\eta)$,

$$\Xi_{0\sigma}(\omega)=\sum_{\vec{k}}\frac{|V_{\vec{k},\sigma}|^2}{\tilde{\omega}-\varepsilon_{\vec{k}}},$$

$$\Xi_{<\sigma}(\omega)=\sum_{\vec{k}}|V_{\vec{k},\sigma}|^2\langle\hat{n}_{\vec{k},\sigma}\rangle\left[\frac{1}{\tilde{\omega}-\varepsilon_{\vec{k}}}+\frac{1}{\tilde{\omega}+\varepsilon_{\vec{k}}-\varepsilon_A}\right],$$

$$\Xi_{1\sigma}(\omega)=\sum_{\vec{k}}|V_{\vec{k},\sigma}|^2\left[\frac{1}{\tilde{\omega}-\varepsilon_{\vec{k}}}+\frac{1}{\tilde{\omega}+\varepsilon_{\vec{k}}-\varepsilon_A}\right]. \tag{27}$$

The correlation functions, $\langle|\sigma\rangle\langle 0|\hat{c}_{\vec{k},\sigma}\rangle_t$ and $\langle|\uparrow,\downarrow\rangle\langle\sigma|\hat{c}_{\vec{k},\bar{\sigma}}\rangle_t$, are determined in the case of equilibrium processes by the Green's functions [Eqs. (23)–(26)] accordingly to the expressions

$$\langle|\sigma\rangle\langle 0|\hat{c}_{\vec{k},\sigma}\rangle=\frac{\mathrm{Im}}{\pi}\int_{-\infty}^{\infty}d\omega f_{<\sigma}(\omega)\frac{V_{k,\sigma}}{\tilde{\omega}-\varepsilon_{\vec{k}}}[G_{\sigma}(\omega)+(-1)^{p_\sigma}G^{c}_{\sigma}(\omega)],$$

$$\langle|\uparrow,\downarrow\rangle\langle\sigma|\hat{c}_{\vec{k},\bar{\sigma}}\rangle=\frac{\mathrm{Im}}{\pi}\int_{-\infty}^{\infty}d\omega f_{<\sigma}(\omega)\frac{V_{\vec{k},\bar{\sigma}}}{\tilde{\omega}-\varepsilon_{\vec{k}}}[G^{\sigma c}_{\uparrow\downarrow}(\omega)+(-1)^{p_{\bar{\sigma}}}G^{\sigma}_{\uparrow\downarrow}(\omega)]. \tag{28}$$

The probability of atomic configurations having either one $(n_{1\sigma})$ or two electrons n_2 is calculated from the corresponding spectral densities, $\rho_\sigma(\omega)=\frac{1}{\pi}\mathrm{Im}\,G_\sigma(\omega)$ and $\rho^{\sigma}_{\uparrow\downarrow}(\omega)=\frac{1}{\pi}\mathrm{Im}\,G^{\sigma}_{\uparrow\downarrow}(\omega)$, as

$$n_{1\sigma}=\langle|\sigma\rangle\langle\sigma|\rangle=\int_{-\infty}^{\infty}d\omega f_{<}(\omega)\rho_\sigma(\omega),$$

$$n_2=\langle|\uparrow\downarrow\rangle\langle\uparrow\downarrow|\rangle=\int_{-\infty}^{\infty}d\omega f_{<}(\omega)\rho^{\sigma}_{\uparrow\downarrow}(\omega), \tag{29}$$

being also valid the following normalization properties:

$$\rightarrow\int_{-\infty}^{\infty}d\omega\rho_\sigma(\omega)=\langle|\sigma\rangle\langle\sigma|\rangle+\langle|0\rangle\langle 0|\rangle,$$

$$\rightarrow\int_{-\infty}^{\infty}d\omega\rho^{\sigma}_{\uparrow\downarrow}(\omega)=\langle|\uparrow\downarrow\rangle\langle\uparrow\downarrow|\rangle+\langle|\sigma\rangle\langle\sigma|\rangle. \tag{30}$$

B. Electron Green's functions

By introducing the identity $\hat{c}_{a,\sigma}=|0\rangle\langle\sigma|+(-1)^{p_\sigma}|\bar{\sigma}\rangle\langle\uparrow,\downarrow|$ in the electron Green's function $G_{a\sigma}(t,t')=i\Theta(t'-t)\langle\{\hat{c}^{\dagger}_{a,\sigma}(t'),\hat{c}_{a,\sigma}(t)\}\rangle$ we obtained the following expression:[39]

$$G_{a\sigma}(\omega)=G_\sigma(\omega)+(-1)^{p_\sigma}G^{c}_{\sigma}(\omega)+(-1)^{p_\sigma}G^{\bar{\sigma}c}_{\uparrow\downarrow}(\omega)+G^{\bar{\sigma}}_{\uparrow\downarrow}(\omega). \tag{31}$$

Then, introducing in Eq. (31) Eqs. (23)–(26) leads to the final expression

$$G_{a\sigma}(\omega)=\frac{1-\langle\hat{n}_{a,\bar{\sigma}}\rangle}{\tilde{\omega}-\varepsilon_I-\Xi_{0\sigma}(\omega)+\dfrac{U\Xi_{<\bar{\sigma}}(\omega)}{\tilde{\omega}-\varepsilon_I-U-\Xi_{0\sigma}(\omega)-\Xi_{1\bar{\sigma}}(\omega)}}+\frac{\langle\hat{n}_{a,\bar{\sigma}}\rangle}{\tilde{\omega}-\varepsilon_I-U-\Xi_{0\sigma}(\omega)+\dfrac{U[\Xi_{<\bar{\sigma}}(\omega)-\Xi_{1\bar{\sigma}}(\omega)]}{\tilde{\omega}-\varepsilon_I-\Xi_{0\sigma}(\omega)-\Xi_{1\bar{\sigma}}(\omega)}}$$
$$+\frac{UI_{\bar{\sigma}}(\omega)}{[\tilde{\omega}-\varepsilon_I-\Xi_{0\sigma}(\omega)][\tilde{\omega}-\varepsilon_I-U-\Xi_{0\sigma}(\omega)-\Xi_{1\bar{\sigma}}(\omega)]+U\Xi_{<\bar{\sigma}}(\omega)}, \tag{32}$$

where $\langle\hat{n}_{a,\sigma}\rangle=n_{1\sigma}+n_2$ is the occupation per spin and the quantity $I_\sigma(\omega)$ has been defined as

$$I_\sigma(\omega)=\sum_{\vec{k}} V^*_{\vec{k},\sigma}\frac{\langle\hat{c}^\dagger_{a,\sigma}\hat{c}_{\vec{k},\sigma}\rangle}{\tilde{\omega}-\varepsilon_{\vec{k}}}-\sum_{\vec{k}} V_{\vec{k},\sigma}\frac{\langle\hat{c}^\dagger_{\vec{k},\sigma}\hat{c}_{a,\sigma}\rangle}{\tilde{\omega}+\varepsilon_{\vec{k}}-\varepsilon_A}. \tag{33}$$

The EOM result [Eq. (32)] leads to a temperature independent Green's function at the particle-hole symmetric point ($\varepsilon_I=-U/2$) of the Anderson model.[41–44] This means that the EOM technique cannot produce the Kondo singularity in the case of the particle-hole symmetric point. It can be shown that the failure of the EOM technique is confined to the imaginary part of the interacting self-energy and to the symmetric point alone.[25] The correct limit behaviors for $V\to 0$ and $U\to 0$ are verified by Eq. (26), and for $U\to\infty$ we found the same expression as in Ref. 24,

$$G_{a\sigma}(\omega)=\frac{1-\langle\hat{n}_{a,\bar{\sigma}}\rangle-I^{U\to\infty}_{\bar{\sigma}}(\omega)}{\tilde{\omega}-\varepsilon_I-\Xi_{0\sigma}(\omega)-\Xi^{U\to\infty}_{<\bar{\sigma}}(\omega)}, \tag{34}$$

where now the quantities $I^{U\to\infty}_{\bar{\sigma}}(\omega)$ and $\Sigma^{U\to\infty}_{<\bar{\sigma}}(\omega)$ correspond to the expressions

$$\Xi^{U\to\infty}_{<\sigma}(\omega)=\sum_{\vec{k}}|V_{\vec{k},\sigma}|^2\langle\hat{n}_{\vec{k},\sigma'}\rangle\frac{1}{\tilde{\omega}-\varepsilon_{\vec{k}}},$$

$$I^{U\to\infty}_{\sigma}(\omega)=\sum_{\vec{k}} V^*_{\vec{k},\sigma}\frac{\langle\hat{c}^\dagger_{a,\sigma}\hat{c}_{\vec{k},\sigma}\rangle}{\tilde{\omega}-\varepsilon_{\vec{k}}}.$$

By considering $I_\sigma(\omega)=0$ in Eq. (32) we recovered the $G_{a\sigma}(\omega)$ calculated by Meir *et al.* within the EOM technique.[10,11] On the other hand, in the pioneer works of Lacroix[12,13] the EOM is truncated accordingly to a scheme in which all the correlation functions originated by a mean-field-like approximation are self-consistently determined. This means in the following case,

$$i\theta(t'-t)\langle\{|\sigma\rangle\langle 0|_{t'};|0\rangle\langle\sigma|\hat{c}^\dagger_{\vec{k}',\sigma}\hat{c}_{k,\sigma'}(t)\}\rangle$$
$$=G_{a\sigma}(t,t')\langle\hat{c}^\dagger_{\vec{k}',\sigma}\hat{c}_{\vec{k},\sigma'}\rangle\delta_{\sigma,\sigma'}+\langle|0\rangle\langle\sigma|\hat{c}^\dagger_{\vec{k}',\sigma}\rangle G_{a\sigma}[\hat{c}_{\vec{k},\sigma'}(t)], \tag{35}$$

that the two correlation functions $\langle\hat{c}^\dagger_{\vec{k}',\sigma}\hat{c}_{\vec{k},\sigma}\rangle$ and $\langle|0\rangle\langle\sigma|\hat{c}^\dagger_{\vec{k}',\sigma}\rangle$ are calculated in a self-consistent way with the Green's functions. The difference with respect to our procedure is that we are using the criterion of closing the EOM by ensuring a strict second-order calculation in the hopping parameter $V_{\vec{k}}$. Hence the correlation functions appearing in Eq. (35) have been calculated up to zero order in $V_{\vec{k}}$, $\langle\hat{c}^\dagger_{\vec{k}',\sigma}\hat{c}_{\vec{k}\sigma}\rangle^0=\langle\hat{n}_{\vec{k},\sigma}\rangle\delta_{\vec{k},\vec{k}'}$; $\langle|0\rangle\langle\sigma|\hat{c}^\dagger_{\vec{k}',\sigma}\rangle^0=0$.

It was found, in the case of an infinite value of U, that the occupation $\langle\hat{n}_{a,\sigma}\rangle$ calculated by using this second order in $V_{\vec{k}}$ criterion was in very good agreement with the exact calculation. It was also found that it is necessary to be consistent with the order in $V_{\vec{k}}$ used to close the equations of motion in order to ensure the total electron number conservation.[24]

III. RESULTS AND DISCUSSION

A. Time-dependent processes

The four-atom system where the exact solution is possible provides a good test of the proposed approximations. In this small system, with four electrons, the linear solid is composed of three atoms and the fourth one is the projectile atom which moves with velocity v. The tight-binding parameters defining the band states of the three-atom linear chain are the site energy $\varepsilon_0=0$ eV and the hopping between nearest neighbors $\beta=2$ eV (see the inset of Fig. 1). The time-dependent coupling between the projectile and the "surface" atom is given by $V=V_0\exp(-2|t|)$. This very discrete level system with only three band states represents the less favorable scenario for the nonperturbed $\langle\hat{n}_{\vec{k},\sigma}\rangle$ assumed in the Green's function calculation [Eq. (10)]. Therefore, if the approximated calculation is able to reproduce satisfactorily the exact results in this case, we would expect a much better agreement with the exact results in the case of a realistic metal surface with a continuum of band states and an electron reservoir behavior.

In Fig. 1(a) it is shown the single per spin $n_{1\sigma}(t)$ and double $n_2(t)$ occupation probabilities of the projectile atom state at the end of the outgoing trajectory for an incoming initial condition $n_2(t_0)=1$. The same is shown in Fig. 1(b) for the case of an incoming positive ion $[n_{1\sigma}(t_0)=n_2(t_0)=0]$.

A very good description of the charge state probabilities is provided by the approximated calculation based on the second order in $V_{\vec{k}}$ criterion to close the equations of motion of the Green's functions [Eqs. (6)–(9)]. The nonperturbed band state occupation $\langle\hat{n}_{\vec{k},\sigma}\rangle^0$ assumed in this approximation is expected to be worst at low velocity values in which the projectile has enough time to "see" the variations. From the comparison shown in Fig. 2, we can conclude that the second order in $V_{\vec{k}}$ approximation practically reproduces the exact results for $V\leq U$.

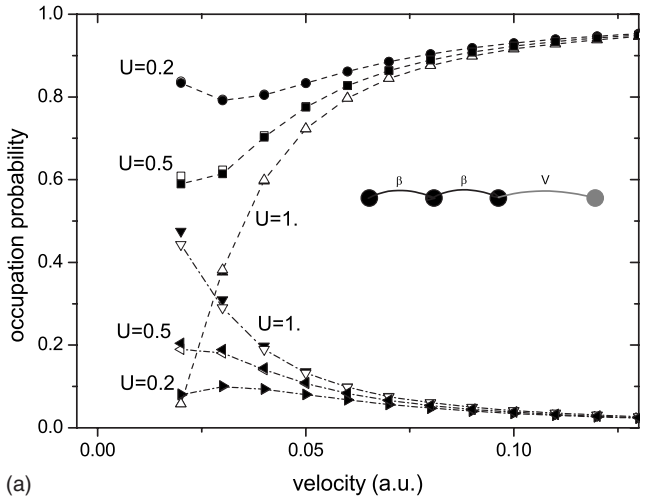

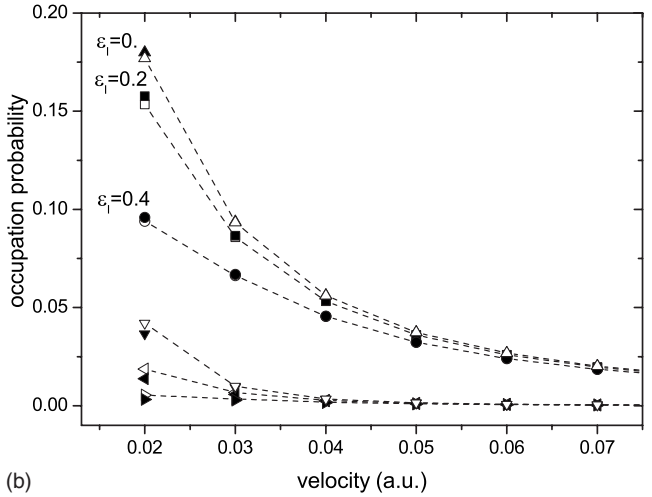

FIG. 1. The probability of single per spin $n_{1\sigma}(\infty)$ (down, left and right triangles) and double $n_2(\infty)$ (up triangles, squares and circles) occupations as a function of the projectile atom velocity. The full symbols correspond to the present work approximation and the empty ones to the exact calculation. (a) For an incoming negative ion $[n_2(t_0)=1]$, $V_0=0.4$ eV, $\varepsilon_I=-1$ eV, and $U=0.2$, 0.5, and 1 eV. (b) For an incoming positive ion $[n_2(t_0)=0,\ n_{1\sigma}(t_0)=0]$, $V_0=0.2$ eV, $U=0.2$ eV, and $\varepsilon_I=0.4$, 0.2, and 0 eV.

In some way the same is observed in Fig. 3 where the case of $V_0 > U$ is shown. For large velocities the projectile tends to exit without changing the incoming state of charge and for low velocities the charge state is defined far from the surface along the outgoing trajectory. In both cases the *effective* coupling term involved is small leading to little variations of the atomic and band state occupations. The second order in $V_{\vec{k}}$ criterion reproduces the exact results in these ranges of velocity values. For intermediate velocities the region closer to the surface is determining the charge states, and in this case the effective coupling term is more significant. It is in this range of velocities where our results differ more appreciably with the exact ones.

This analysis allows us to conclude that the Green's functions [Eqs. (6)–(9)] determined by the EOM method using the second order in $V_{\vec{k}}$ criterion are very appropriate to treat correlated atom states in dynamical processes for values of the electronic repulsion U going from 0 to ∞ and for couplings with the band states $V_{\vec{k}} \leq U$.

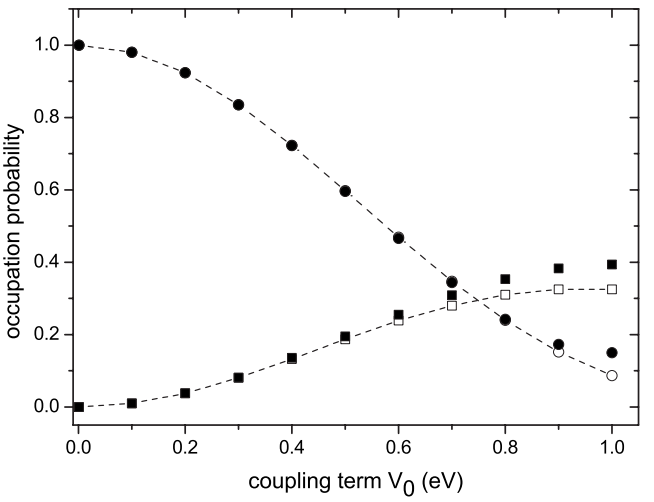

FIG. 2. The probability of single per spin (squares) and double (circles) occupations as a function of the coupling strength V_0. The full symbols correspond to the present work approximation and the empty ones to the exact calculation. For a negative incoming ion with velocity $v=0.05$ u.a., $\varepsilon_I=-1$ eV, $U=1$ eV.

In this very discrete four level system, the assumption of nonperturbed average band state occupation numbers $\langle \hat{n}_{\vec{k},\sigma} \rangle^0$ may not work very well for small atom velocities. This is not the case of a real solid with a continuum of band states where the mean-field approximation $\langle \hat{n}_{\vec{k},\sigma} \rangle^0$ is completely plausible. At large enough atom velocities this assumption is more valid in any case, and the second order in V_{k} becomes a better approximation to the exact calculation since the fine details of the electronic structure of the interacting system are smeared out by the dynamical process associated with the interaction time value involved.

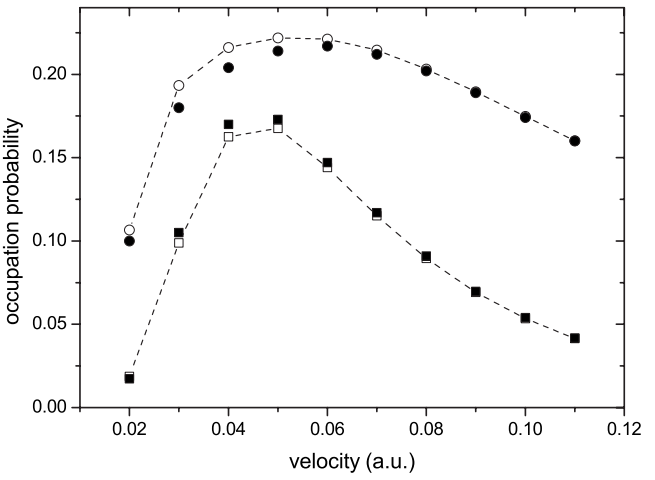

FIG. 3. The single per spin (circles) and double (squares) occupation probabilities as a function of the projectile atom velocity. The full symbols correspond to the present work approximation and the empty ones to the exact calculation. For an incoming positive ion, $n_2(t_0)=0$, $n_{1\sigma}(t_0)=0$, $V_0=1$ eV, $U=0.2$ eV, and $\varepsilon_I=-1$ eV.

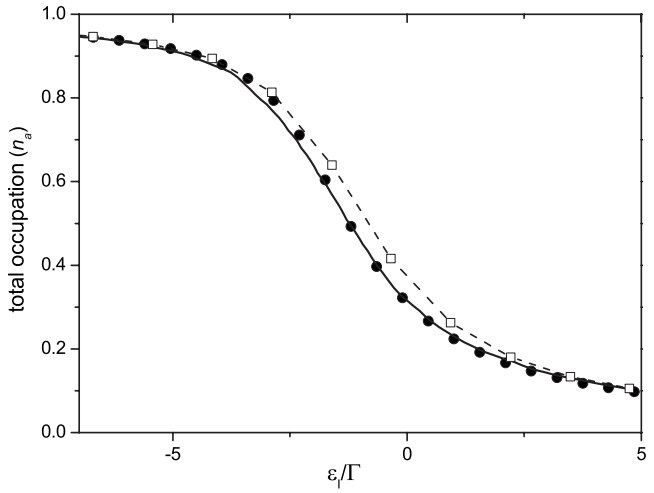

FIG. 4. The occupation $\langle \hat{n}_a \rangle$ in the infinite U limit as a function of ε_l/Γ. The full circles are the present calculation [Eq. (34)] and the empty square symbols correspond to the calculation in Refs. 12 and 25. The solid line is the exact calculation from Ref. 16.

B. Equilibrium processes

In the following a flat-band of half-width D is assumed for the surface, and the constant level width $\Gamma = \pi \Sigma_{\tilde{k}} |V_{\tilde{k}}|^2 \delta(\varepsilon - \varepsilon_{\tilde{k}}) = \pi \rho_0 V^2$ is introduced.

The excellent agreement of the second order in $V_{\tilde{k}}$ calculation of the occupation $\langle \hat{n}_a \rangle = \Sigma_\sigma \langle \hat{n}_{a,\sigma} \rangle$ with the exact results in the case of an infinite value of U has been discussed in a previous work.[24] In Fig. 4 we show our results for the occupation as a function of ε_l/Γ in the limit $U \to \infty$ compared with the exact ones and those obtained within the approximation of Lacroix.[12,25]

For finite values of $U(U/\pi\Gamma=4)$, our calculation of the dependence of the total occupation, $\langle n_a \rangle = 2n_2 + n_{1\uparrow} + n_{1\downarrow}$, with the temperature leads to a qualitatively correct behavior, as it is observed in Fig. 5 from the comparison with the RGT

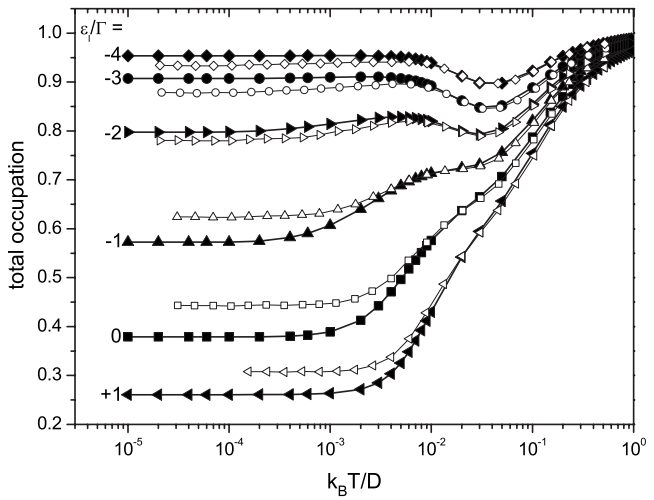

FIG. 5. The total occupation $2(n_{1\sigma}+n_2)$ as a function of the temperature for $\Gamma=0.01D$, $U/\pi\Gamma=4$, and different values of ε_l/Γ. The full symbols correspond to the present work calculation and the empty ones to the exact results from Ref. 16.

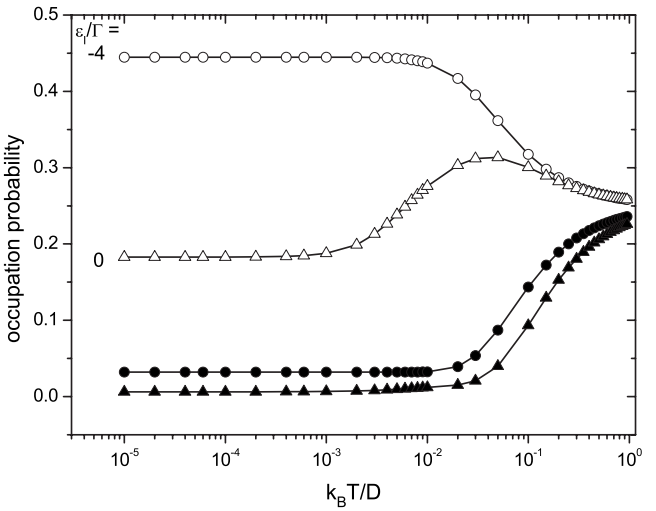

FIG. 6. The probabilities of charge configurations with one electron (empty symbols) and two electrons (full symbols) as a function of the temperature for $\Gamma=0.01D$, $U/\pi\Gamma=4$. Two values of ε_l/Γ: −4 (circles) and 0 (triangles) are shown.

exact results[16] for different values of the energy level (ε_l/Γ) position. Our approximation at low temperatures is better in the Kondo-like regime, $\varepsilon_l/\Gamma < -1$, and it shows a little more pronounced variation with the temperature than the exact calculation in the case of a mixed valence regime $(\varepsilon_l/\Gamma \approx 0)$.

In Fig. 6 it is discriminated the contributions to the total occupation coming from the single charged $(n_{1\sigma})$ and double charged (n_2) configurations. The single charged configurations are the most probable for this U/Γ relation and within a realistic range of temperature values $(k_B T/D \leq 0.01)$. The double occupation becomes more important as lower ε_l/Γ is; this is in the Kondo regime. The correct infinite temperature limit is well reproduced by our calculation; all the charge state configurations have the same probability in this limit (0.25).

In Fig. 7 we compare the total occupation calculated by using the second order in $V_{\tilde{k}}$ approximation with the corresponding results obtained by neglecting in Eq. (32) the term $I_\sigma(\omega)$ given by Eq. (33). It is also shown in this figure the comparison with exact results obtained from the RGT calculation. To neglect the *crossed terms* such as $\langle \hat{c}^\dagger_{a,\sigma} \hat{c}_{\tilde{k},\sigma} \rangle$ is an approximation widely used in previous works.[10,11,23,26] We can observe from Fig. 7 that it is only a good approximation for very large temperatures. To conserve the crossed terms within a strict second order in V calculation provides clearly a better approximation, being the difference with respect to neglect the crossed terms more pronounced in the mixed valence regime.

In Figs. 8(a)–8(c) the corresponding density of states calculated in the cases $\varepsilon_l/\Gamma = -3; -1; 1$ is compared with the exact results for several temperature values. Our calculation based on a weak coupling criterion leads to energy positions of the two resonances nearer to the isolated atom values (ε_l and $\varepsilon_l + U$) and also to smaller widths compared with the RGT calculation.[16] As it is observed from the insets of Fig. 8, the density of states at the Fermi level $\rho(0,T)$ follows the

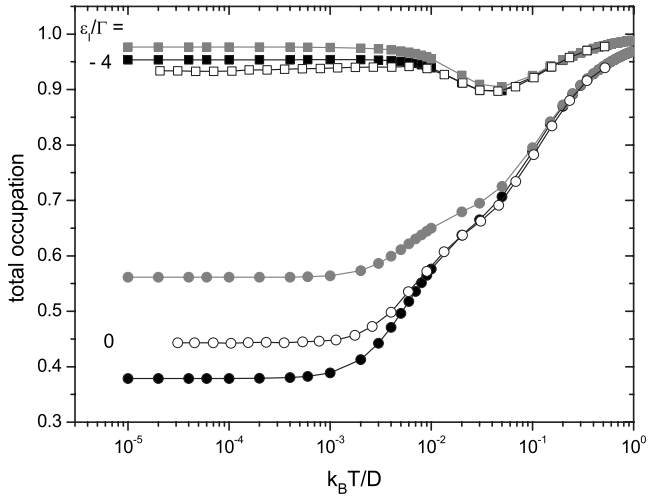

FIG. 7. The total occupation as a function of the temperature for $\Gamma=0.01D$, $U/\pi\Gamma=4$. Two values of ε_I/Γ: −4 and 0 are shown. Full black symbols correspond to the present work calculation; the full gray symbols were obtained by considering $I_\sigma(\omega)=0$ in Eq. (32). The exact results are also included (empty symbols).

same behavior with temperature as the exact results in the case of Kondo and valence mixed regimes, while it shows practically an opposite dependence in the case of an empty orbital regime.

The change of behavior from a weak coupling strength to a strong one can be seen in Fig. 9(a) where the total occupation $(2n_2+n_{1\uparrow}+n_{1\downarrow})$ is shown as a function of $(\varepsilon_I/U+1/2)$ for different values of Γ/U. For $\Gamma/U\geq 0.3$ the total occupation behaves almost linearly with $(\varepsilon_I/U+1/2)$, whereas for weak coupling strengths $(\Gamma/U<0.3)$ the energy dependence develops a plateau around the symmetric point $\varepsilon_I=-U/2$. This change of behavior is due to the fact that the extent of the local moment regime centered on $\varepsilon_I/U+1/2=0$ increases when Γ/U decreases. A "staircase" variation of the total occupation with the energy level is finally obtained in the localized regime $\Gamma/U\to 0$. The presented results are qualitatively very similar to those obtained by a numerical solution of the Bethe ansatz equations[32] in the same range of parameter values.

In Fig. 9(b) we can observe that the probabilities of single occupation per spin $(n_{1\sigma})$ and of double occupation (n_2) change abruptly as a function of $\varepsilon_I/U+1/2$ for small values of Γ/U. In this case the variation of the number of electrons in the atom state occurs practically in integer quantities (from two to one and from one to zero electrons). In the case of strong coupling strengths, the probabilities present a continuous variation with $\varepsilon_I/U+1/2$, and the total occupation acquires in this form fractional values.

A key ingredient of the Kondo effect is the phase shift given by $\delta=\pi n_a$ at $T=0$ K that an electron undergoes when it crosses the dot (where n_a is the total occupation in the dot or atom). Its direct measurement became feasible recently in quantum dots via Aharonov-Bohm interferometery.[33–35] In Fig. 10 we show experimental results corresponding to two cases, the *unitary limit* where the phase shift climbs almost linearly with the gate potential V_G and the usually called *Kondo regime*, at a smaller value of the coupling strength,

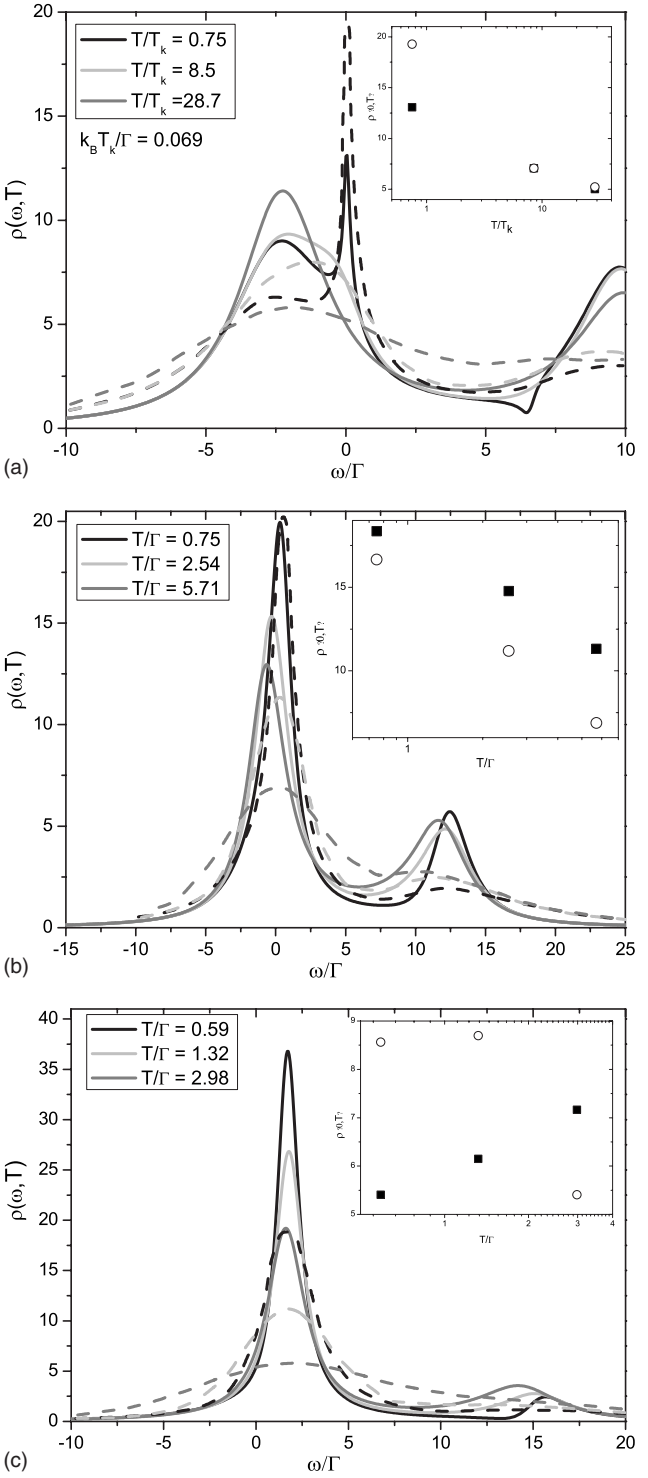

FIG. 8. The density of states projected on the atom as a function of ω/Γ for $\Gamma=0.01D$ $U/\pi\Gamma=4$ and for different temperature values. (a) $\varepsilon_I/\Gamma=-3$; (b) $\varepsilon_I/\Gamma=-1$; and (c) $\varepsilon_I/\Gamma=1$. The solid curves are our results and the dashed curves are exact results from Ref. 16. In the inset it is compared the temperature dependence of the density of states at the Fermi level; the squares are our results and the circles are the exact ones.

where the phase shift develops a wide plateau at almost π.[32,33] The experimental data can be fitted with two parameters, Γ/U and ε_I, being the value of ε_I governed by the

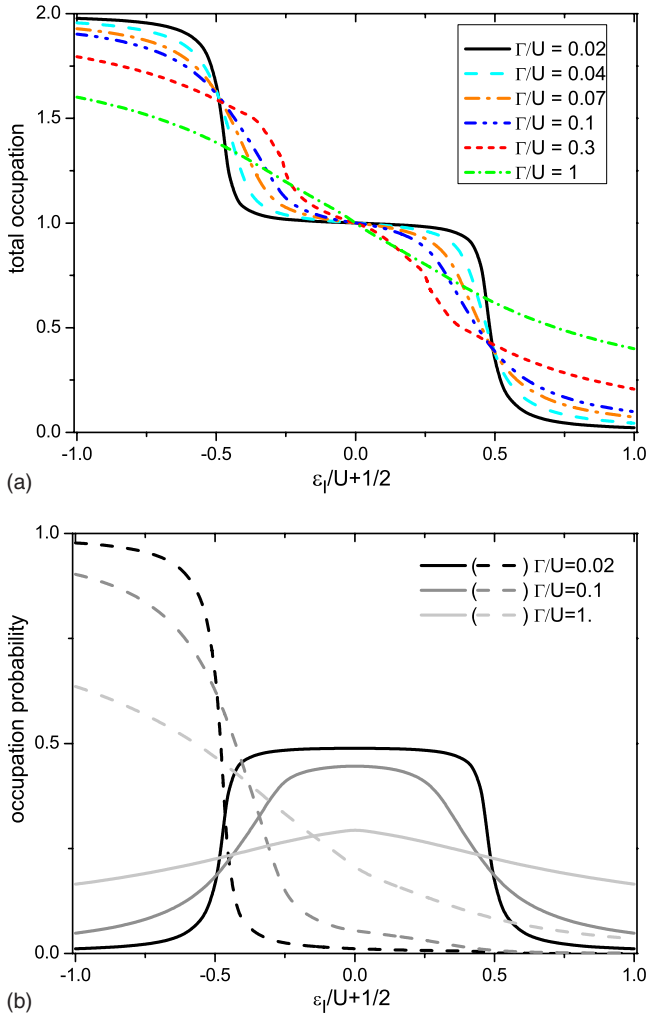

FIG. 9. (Color online) (a) Total occupation as a function of $\varepsilon_l/U+1/2$ for different values of Γ/U. (b) The same for single (solid lines) and double (dashed lines) occupation probabilities.

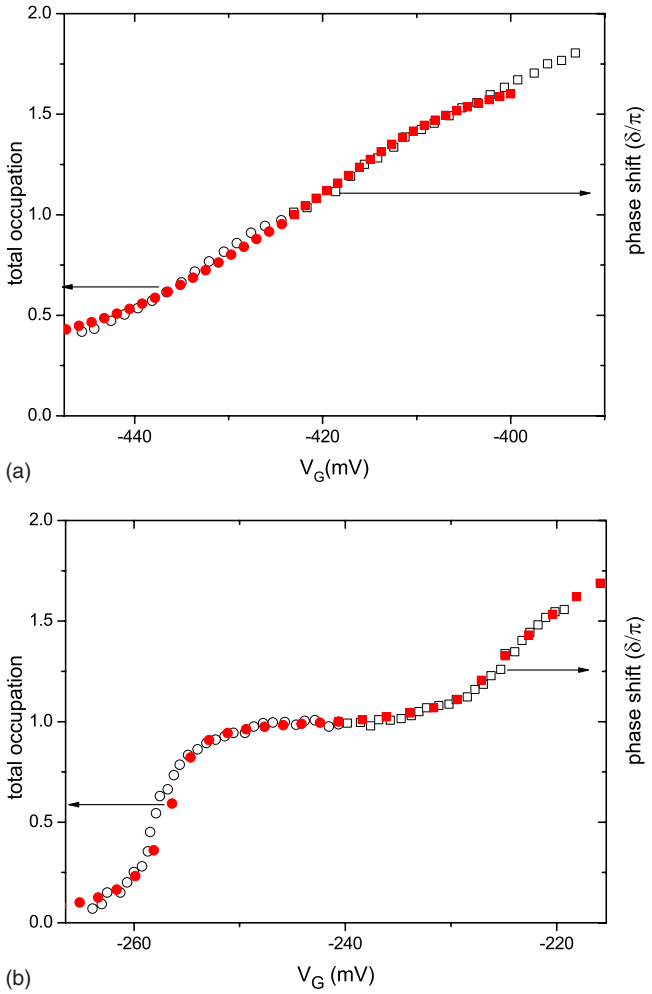

FIG. 10. (Color online) The calculated total occupation and the measured phase shift δ as a function of the gate voltage V_G. (a) Unitary limit. Our theoretical results at $\Gamma/U=1$ (full symbols) compared to the experimental data from Ref. 33 (empty symbols). (b) Kondo regime. The same is shown with $\Gamma/U=0.04$ (below) and 0.1 (above). The same shifts in Ref. 32 are considered in the δ scale.

strength of the gate voltage. By fitting the experimental data from our results presented in Fig. 9(a) we found the best fitting value of Γ/U in the different regimes [a linear correspondence between V_G and $\varepsilon_l/U+1/2$ is assumed with $\Delta V_G/\Delta(\varepsilon_l/U+1/2)\approx 35$ mV].

The best fit is obtained for $\Gamma/U=1$ in the unitary limit both below and above the symmetric limit and in the Kondo regime for $\Gamma/U=0.04$ and 0.1 (below and above the symmetric limit, respectively). These values are in very good qualitative agreement with those obtained by using the Bethe ansatz equations in the case of the Kondo regime, $\Gamma/U=0.04$ and 0.07.[32] But in the case of the unitary limit where a stronger coupling is involved, our calculation requires a Γ/U twice the one used in Ref. 32.

In the case of larger temperature values, $T\geq\Gamma$, the phase shift that determines the oscillations of the conductance is calculated as $\delta=\arg(t_{a\sigma})$, where $t_{a\sigma}$ is the thermally averaged transmission amplitude given by $t_{a\sigma}=\Gamma\int d\varepsilon(\partial f_<(\partial\varepsilon)G_{a\sigma}(\varepsilon)$.[34] In Fig. 11 we show the phase shift in this form calculated by using expression (32) for the Green's function $G_{a\sigma}(\varepsilon)$ as a function of $(\varepsilon_l/U+1/2)$ for three values of Γ/U.

For small values of Γ/U we observe the pronounced rises of δ by almost π with a pronounced phase lapse in the valley in between. This behavior is consistent with the well defined Coulomb-blockade peaks experimentally observed in the gate potential dependence of $|t_{a\sigma}|$.[45] The larger the Γ/U, the less sharp these feature since the peaks increasingly overlap.

We can observe from Fig. 11 that for $T=\Gamma$ the neglect of the crossed term $\langle\hat{c}^\dagger_{a,\bar{\sigma}}\hat{c}_{\tilde{k},\bar{\sigma}}\rangle$ in the $G_{a\sigma}(\varepsilon)$ calculation [Eq. (32)] leads to practically the same results of the complete calculation.

IV. CONCLUSIONS

We presented a theoretical proposal for treating localized and strong interacting electrons in atoms which are either static or moving near to a surface. The most probable charge state configurations in each case are introduced and manipulated by an adequate projection technique and their probabilities of occurrence calculated by using the Keldysh-

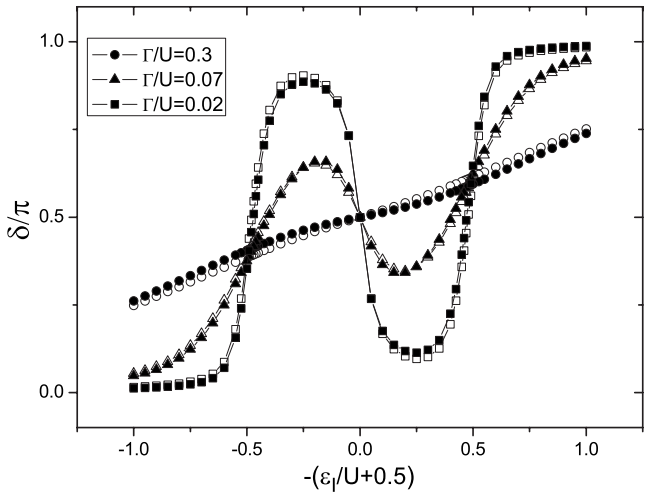

FIG. 11. Phase of $t_{a\sigma}$ (see text) as a function of $(\varepsilon_I/U+1/2)$ for three values of Γ/U and $T=\Gamma$. Full symbols correspond to the calculation by using Eq. (32). Empty symbols are calculated by considering $I_\sigma(\omega)=0$ in Eq. (32).

Green functions. The equations of motion of these Green's functions are solved within a second order in the hopping with the band states. In this way the knowledge of both the time-dependent and the energy-dependent Green's functions allows us to solve a great variety of processes such as chemisorption, electronic transport through nanodevices (atoms, molecules, and quantum dots), and atom-surface collision. Nevertheless this is an approximated calculation; its potentiality resides in the applicability to interacting systems which incorporate very important ingredients such as the proper electronic structure of atoms and surfaces. The results presented in this work show that our proposal provides a qualitatively correct description of charge exchange processes in the stationary case, while in the case of dynamical situations the agreement with exact results is amazing, taking into account the not very appropriate discrete nature of the four level system used to test the proposed approximation. In any case the second-order approximation can reach the exact results within a dynamical process due to the large number of electronic configurations involved in the time evolution.

ACKNOWLEDGMENTS

We thank R. Monreal for many interesting discussions. One of the authors (E.C.G.) acknowledges financial support by ANPCyT through Grant No. PICT-2007-00811 and U.N.L. through the CAI+D Project No. PI-68-348. F.F. has been supported by the Spanish CICYT under Projects No. MAT2007-60966 and No. NAN-2004-09183C-10-07 and the CAM under Project No. 0505/MAT/0303.

APPENDIX

Let us see the details of the EOM applied to the calculation of the Green's function [Eq. (6)]. The equations of motion of the higher-order Green's functions that appear in Eq. (10) are closed by employing the mean-field approximations given by Eq. (11). In this way the following equations of motion are obtained for these higher-order Green's functions:

$$i\frac{dG_\sigma(|0\rangle\langle 0|\hat{c}_{\vec{k},\sigma})}{dt} = \delta(t'-t)\langle|\sigma\rangle\langle 0|\hat{c}_{\vec{k},\sigma}\rangle_{t'} + \varepsilon_{\vec{k}}G_\sigma(|0\rangle\langle 0|\hat{c}_{\vec{k},\sigma}) + V_{\vec{k},\sigma}\langle 1-\hat{n}_{\vec{k},\sigma}\rangle G_\sigma(t,t'),$$

$$i\frac{dG_\sigma(|\sigma'\rangle\langle\sigma|\hat{c}_{\vec{k},\sigma'})}{dt} = -\delta(t'-t)\langle|\sigma'\rangle\langle 0|\hat{c}_{\vec{k},\sigma'}\rangle_{t'} + \varepsilon_{\vec{k}}G_\sigma(|\sigma'\rangle\langle\sigma|\hat{c}_{\vec{k},\sigma'}) + V_{\vec{k},\sigma'}\langle\hat{n}_{\vec{k},\sigma'}\rangle G_\sigma(t,t') + (-1)^{p_{\bar\sigma}}\delta_{\sigma',\bar\sigma}V_{\vec{k},\bar\sigma}\langle 1-\hat{n}_{\vec{k},\bar\sigma}\rangle G_\sigma(|\sigma'\rangle\langle\uparrow,\downarrow|),$$

$$i\frac{dG_\sigma(|0\rangle\langle\uparrow,\downarrow|\hat{c}^\dagger_{\vec{k},\bar\sigma})}{dt} = \delta(t'-t)\langle|\sigma\rangle\langle\uparrow,\downarrow|\hat{c}^\dagger_{\vec{k},\bar\sigma}\rangle_{t'} - (\varepsilon_{\vec{k}}-\varepsilon_A)G_\sigma(|0\rangle\langle\uparrow,\downarrow|\hat{c}^\dagger_{\vec{k},\bar\sigma}) - V^*_{\vec{k},\bar\sigma}\langle 1-\hat{n}_{\vec{k},\bar\sigma}\rangle G_\sigma(|\bar\sigma\rangle\langle\uparrow,\downarrow|) - (-1)^{p_{\bar\sigma}}V^*_{\vec{k},\bar\sigma}\langle\hat{n}_{\vec{k},\bar\sigma}\rangle G_\sigma(t,t').$$

By integrating these ones and then replacing the result in Eq. (10) the final expression of the equation of motion for $G_\sigma(t,t')$ given by Eq. (12) is obtained. In the same way we arrived to the equation of motion for $G^\sigma_{\uparrow\downarrow}(t,t')$ given by Eq. (13).

The equations of motion for the crossed Green's functions [Eq. (16)] are calculated by following an analogous procedure:

$$i\frac{dG^c_\sigma(t,t')}{dt} = (\varepsilon_A-\varepsilon_I)G^c_\sigma(t,t') - i\theta(t'-t)(-1)^{p_{\bar\sigma}}\sum_{\vec{k}} D^{\bar\sigma}_{1\vec{k}}(t,t') + \int_{-\infty}^{\infty} d\tau[\Xi^A_{0\sigma}+\Xi^A_{1\bar\sigma}-\Xi^A_{<\bar\sigma}]G^c_\sigma + (-1)^{p_{\bar\sigma}}\int_{-\infty}^{\infty} d\tau\Xi^A_{<\bar\sigma}G_\sigma, \tag{A1}$$

$$i\frac{dG^{\sigma c}_{\uparrow\downarrow}(t,t')}{dt} = \varepsilon_I G^{\sigma c}_{\uparrow\downarrow}(t,t') + i\theta(t'-t)(-1)^{p_\sigma}\sum_{\vec{k}} D^{\sigma}_{2\vec{k}}(t,t') + \int_{-\infty}^{\infty} d\tau[\Xi^A_{0\bar\sigma}+\Xi^A_{<\sigma}]G^{\sigma c}_{\uparrow\downarrow} + (-1)^{p_\sigma}\int_{-\infty}^{\infty} d\tau[\Xi^A_{1\sigma}-\Xi^A_{<\sigma}]G^{\sigma}_{\uparrow\downarrow}. \tag{A2}$$

The expressions of the different quantities $D^\sigma_{i\vec{k}}(t,t')$ and $\Xi^A_j(t,\tau)$ appearing in Eqs. (A1) and (A2) are those given by Eqs. (17) and (18), respectively.

Now we show the details of the EOM method applied to the calculation of the F-like Green's functions. In the case of the Green's function given by Eq. (8) we have

$$i\frac{dF_\sigma(t,t')}{dt} = \varepsilon_I F_\sigma(t,t') + \sum_{\vec{k}} V^*_{\vec{k},\sigma} F_\sigma(|0\rangle\langle 0|\hat{c}_{\vec{k},\sigma}) + \sum_{\vec{k},\sigma'} V^*_{\vec{k},\sigma'} F_\sigma(|\sigma'\rangle\langle\sigma|\hat{c}_{\vec{k},\sigma'}) - (-1)^{p_{\bar{\sigma}}}\sum_{\vec{k}} V_{\vec{k},\bar{\sigma}} F_\sigma(|0\rangle\langle\uparrow,\downarrow|\hat{c}^\dagger_{\vec{k},\bar{\sigma}}). \quad \text{(A3)}$$

We consider the same mean-field approximations as in the case of the G-like functions in order to close the infinite hierarchy equations of motion by using a strict second order in $V_{\vec{k}}$ criterion. In this way we arrived to the final equations of motion for the new F functions of the type $F_A(|B\rangle\langle C|\hat{c}_{\vec{k},\sigma}) = i\langle[A(t'),|B\rangle\langle C|\hat{c}_{\vec{k},\sigma}(t)]\rangle$ appearing in Eq. (A3),

$$i\frac{dF_\sigma(|0\rangle\langle 0|\hat{c}_{\vec{k},\sigma})}{dt} = \varepsilon_{\vec{k}} F_\sigma(|0\rangle\langle 0|\hat{c}_{\vec{k},\sigma}) + V_{\vec{k},\sigma}\langle 1-\hat{n}_{\vec{k},\sigma}\rangle F_\sigma(t,t'),$$

$$i\frac{dF_\sigma(|\sigma'\rangle\langle\sigma|\hat{c}_{\vec{k},\sigma'})}{dt} = \varepsilon_{\vec{k}} F_\sigma(|\sigma'\rangle\langle\sigma|\hat{c}_{\vec{k},\sigma'}) + V_{\vec{k},\sigma'}\langle\hat{n}_{\vec{k},\sigma'}\rangle F_\sigma(t,t') + (-1)^{p_{\bar{\sigma}}}\delta_{\sigma',\bar{\sigma}} V_{\vec{k},\bar{\sigma}}\langle 1-\hat{n}_{\vec{k},\bar{\sigma}}\rangle F_\sigma(|\sigma'\rangle \times\langle\uparrow,\downarrow|),$$

$$i\frac{dF_\sigma(|0\rangle\langle\uparrow,\downarrow|\hat{c}^\dagger_{\vec{k},\bar{\sigma}})}{dt} = -(\varepsilon_{\vec{k}}-\varepsilon_A)F_\sigma(|0\rangle\langle\uparrow,\downarrow|\hat{c}^\dagger_{\vec{k},\bar{\sigma}}) - V^*_{\vec{k},\bar{\sigma}}\langle 1-\hat{n}_{\vec{k},\bar{\sigma}}\rangle F_\sigma(|\bar{\sigma}\rangle\langle\uparrow,\downarrow|) - (-1)^{p_{\bar{\sigma}}} V^*_{\vec{k},\bar{\sigma}}\langle\hat{n}_{\vec{k},\bar{\sigma}}\rangle F_\sigma(t,t').$$

These equations have to be integrated in this case from the time value $t_0\to-\infty$ for which there is no interaction and then replaced in Eq. (A3). By taking into account the following initial conditions ($t=t_0$) valid for the F-like Green's functions,

$$F_A[|B\rangle\langle C|\hat{c}_{\vec{k},\sigma}(t_0)] = [2\langle\hat{n}_{\vec{k},\sigma}\rangle - 1]G_A[|B\rangle\langle C|\hat{c}_{\vec{k},\sigma}(t_0)],$$

we arrived finally to Eq. (14) and in the same way to Eq. (15) and to the following equations of motion for the crossed F-like Green's functions,

$$i\frac{dF^c_\sigma(t,t')}{dt} = -(\varepsilon_I-\varepsilon_A)F^c_\sigma(t,t') - i\theta(t'-t_0)(-1)^{p_{\bar{\sigma}}} \times\sum_{\vec{k}}[2\langle\hat{n}_{\vec{k},\bar{\sigma}}\rangle - 1]D^{\bar{\sigma}}_{1\vec{k}}(t,t') + \int_{-\infty}^{\infty} d\tau[\Xi^A_{0\sigma} + \Xi^A_{1\bar{\sigma}} - \Xi^A_{<\bar{\sigma}}]F^c_\sigma + (-1)^{p_{\bar{\sigma}}}\int_{-\infty}^{\infty} d\tau\Xi^R_{<\bar{\sigma}}F_\sigma + \int_{-\infty}^{\infty} d\tau[\Omega_{0\sigma}+\Omega_{1\bar{\sigma}}-\Omega_{<\bar{\sigma}}]G^c_\sigma + (-1)^{p_{\bar{\sigma}}}\int_{-\infty}^{\infty} d\tau\Omega_{<\bar{\sigma}}G_\sigma, \quad \text{(A4)}$$

$$i\frac{dF^{\sigma c}_{\uparrow\downarrow}(t,t')}{dt} = \varepsilon_I F^{\sigma c}_{\uparrow\downarrow}(t,t') + i\theta(t'-t_0)(-1)^{p_\sigma}\sum_{\vec{k}}[2\langle\hat{n}_{\vec{k},\sigma}\rangle - 1]D^\sigma_{2\vec{k}}(t,t') + \int_{-\infty}^{\infty} d\tau[\Xi^R_{0\bar{\sigma}} + \Xi^R_{<\sigma}]F^{\sigma c}_{\uparrow\downarrow} + (-1)^{p_\sigma}\int_{-\infty}^{\infty} d\tau[\Xi^R_{1\sigma} - \Xi^R_{<\sigma}]F^\sigma_{\uparrow\downarrow} + \int_{-\infty}^{\infty} d\tau[\Omega_{0\bar{\sigma}}+\Omega_{<\sigma}]G^{\sigma c}_{\uparrow\downarrow} + (-1)^{p_\sigma}\int_{-\infty}^{\infty} d\tau[\Omega_{1\sigma}-\Omega_{<\sigma}]G^\sigma_{\uparrow\downarrow}. \quad \text{(A5)}$$

In all the cases it is verified $\Xi^R(t,\tau) = [\Xi^A(\tau,t)]^*$, and the expressions of the Ω-like self-energies appearing in the differential equations of the F-Green's functions are given by Eq. (19).

The G-like functions are integrated from t' to $t\le t'$ and the F functions from t_0 to $t\ge t_0$ by using the following initial conditions:

$$F_\sigma(t_0,t') = \begin{cases} +G_\sigma(t_0,t') \\ -G_\sigma(t_0,t') \end{cases} \quad \text{if}\langle|\sigma\rangle\langle\sigma|\rangle_{t_0} = \begin{cases} 1/2 \\ 0, \end{cases}$$

$$F^\sigma_{\uparrow\downarrow}(t_0,t') = \begin{cases} +G^\sigma_{\uparrow\downarrow}(t_0,t') \\ -G^\sigma_{\uparrow\downarrow}(t_0,t') \end{cases} \quad \text{if}\langle|\uparrow\downarrow\rangle\langle\uparrow\downarrow|\rangle_{t_0} = \begin{cases} 1 \\ 0, \end{cases}$$

$$F^{\sigma c}_{\uparrow\downarrow}(t_0,t') = \begin{cases} +G^{\sigma c}_{\uparrow\downarrow}(t_0,t') \\ -G^{\sigma c}_{\uparrow\downarrow}(t_0,t') \end{cases} \quad \text{if}\langle|\sigma\rangle\langle\sigma|\rangle_{t_0} = \begin{cases} 1/2 \\ 0, \end{cases}$$

$$F^c_\sigma(t_0,t') = \begin{cases} +G^c_\sigma(t_0,t') \\ -G^c_\sigma(t_0,t') \end{cases} \quad \text{if}\langle|\uparrow\downarrow\rangle\langle\uparrow\downarrow|\rangle_{t_0} = \begin{cases} 1 \\ 0. \end{cases}$$

The F functions require to know the G functions from t' to t_0 and both of them require to know correlation functions such as the average occupations $(\langle|\sigma\rangle\langle\sigma|\rangle_t, \langle|\uparrow\downarrow\rangle\langle\uparrow\downarrow|\rangle_t)$ and the average crossed terms $\langle|\sigma\rangle\langle 0|\hat{c}_{\vec{k},\sigma}\rangle_t$ and $\langle|\uparrow,\downarrow\rangle\langle\sigma|\hat{c}_{\vec{k},\bar{\sigma}}\rangle_t$ at the final time value $t=t'$. Hence we need a *guess* value of the average crossed terms to begin the calculation of the Green's functions. This guess value is obtained by considering the following mean-field-like approximation to the equation of motion of these terms:

$$i\frac{dC^1_{\vec{k}}}{dt} = V_{\vec{k},\sigma}[\langle \hat{n}_{1\sigma}\rangle - \langle \hat{n}_{\vec{k},\sigma}\rangle\langle 1-\hat{n}_{1\bar{\sigma}}-\hat{n}_2\rangle]e^{i\varepsilon_{\vec{k}}(t-t_0)} \times \exp\left(-i\int_{t_0}^{t}\varepsilon_I dx\right), \quad \text{(A6)}$$

$$i\frac{dC^2_{\vec{k}}}{dt} = (-1)^{p_{\bar{\sigma}}}V_{\vec{k},\bar{\sigma}}[\langle 1-\hat{n}_{\vec{k},\bar{\sigma}}\rangle\langle \hat{n}_2\rangle - \langle \hat{n}_{\vec{k},\bar{\sigma}}\rangle\langle \hat{n}_{1\sigma}\rangle]e^{i\varepsilon_{\vec{k}}(t-t_0)} \times \exp\left[-i\int_{t_0}^{t}(\varepsilon_A-\varepsilon_I)dx\right], \quad \text{(A7)}$$

where it has been introduced the quantities

$$C^1_{\vec{k}} = \langle|\sigma\rangle\langle 0|\hat{c}_{\vec{k},\sigma}\rangle e^{i\varepsilon_{\vec{k}}(t-t_0)}\exp\left(-i\int_{t_0}^{t}\varepsilon_I dx\right),$$

$$C^2_{\vec{k}} = \langle|\uparrow,\downarrow\rangle\langle\sigma|\hat{c}_{\vec{k},\bar{\sigma}}\rangle e^{i\varepsilon_{\vec{k}}(t-t_0)}\exp\left[-i\int_{t_0}^{t}(\varepsilon_A-\varepsilon_I)dx\right].$$

The crossed terms at each time value t are in this way calculated by using the time derivative expressions (A6) and (A7) from the values of the crossed terms at $t-dt$ recalculated with expression (22).

[1] P. W. Anderson, Phys. Rev. **124**, 41 (1961).
[2] D. N. Zubarev, Usp. Fiz. Nauk **71**, 71 (1960) [Sov. Phys. Usp. **3**, 320 (1960)].
[3] K. G. Wilson, Rev. Mod. Phys. **47**, 773 (1975).
[4] H. R. Krishna-murthy, J. W. Wilkins, and K. G. Wilson, Phys. Rev. B **21**, 1044 (1980).
[5] N. Kawakami and A. Okiji, J. Phys. Soc. Jpn. **51**, 2043 (1982).
[6] N. Kawakami and A. Okiji, J. Phys. Soc. Jpn. **51**, 1145 (1982).
[7] A. M. Tsvelick and P. B. Wiegmann, Adv. Phys. **32**, 453 (1983).
[8] M. Jarrell, J. E. Gubernatis, and R. N. Silver, Phys. Rev. B **44**, 5347 (1991).
[9] R. N. Silver, J. E. Gubernatis, D. S. Sivia, and M. Jarrell, Phys. Rev. Lett. **65**, 496 (1990).
[10] Y. Meir, N. S. Wingreen, and P. A. Lee, Phys. Rev. Lett. **66**, 3048 (1991).
[11] Y. Meir, N. S. Wingreen, and P. A. Lee, Phys. Rev. Lett. **70**, 2601 (1993).
[12] C. Lacroix, J. Phys. F: Met. Phys. **11**, 2389 (1981).
[13] C. Lacroix, J. Appl. Phys. **53**, 2131 (1982).
[14] T.-K. Ng, Phys. Rev. Lett. **76**, 487 (1996).
[15] Q.-F. Sun and T.-H. Lin, J. Phys.: Condens. Matter **9**, 4875 (1997); C. Niu, D. L. Lin, and T.-H. Lin, *ibid.* **11**, 1511 (1999).
[16] T. A. Costi, A. C. Hewson, and V. Zlatic, J. Phys.: Condens. Matter **6**, 2519 (1994).
[17] S. Hershfield, J. H. Davies, and J. W. Wilkins, Phys. Rev. Lett. **67**, 3720 (1991); Phys. Rev. B **46**, 7046 (1992).
[18] K. Yosida and K. Yamada, Prog. Theor. Phys. **46**, 244 (1970).
[19] V. Zlatic and B. Horvatic, Phys. Rev. B **28**, 6904 (1983).
[20] A. Levy Yeyati, A. Martín-Rodero, and F. Flores, Phys. Rev. Lett. **71**, 2991 (1993).
[21] M. Krawiec and K. I. Wysokiński, Phys. Rev. B **66**, 165408 (2002).
[22] A. D. Güçlü, Q.-F. Sun, and H. Guo, Phys. Rev. B **68**, 245323 (2003).
[23] R. Swirkowicz, J. Barnas, and M. Wilczynski, Phys. Rev. B **68**, 195318 (2003).
[24] E. C. Goldberg, F. Flores, and R. C. Monreal, Phys. Rev. B **71**, 035112 (2005).
[25] V. Kashcheyevs, A. Aharony, and O. Entin-Wohlman, Phys. Rev. B **73**, 125338 (2006).
[26] M. Galperin, A. Nitzan, and M. A. Ratner, Phys. Rev. B **76**, 035301 (2007).
[27] Y. Qi, J.-X. Zhu, S. Zhang, and C. S. Ting, Phys. Rev. B **78**, 045305 (2008).
[28] M. A. Romero and E. C. Goldberg, Phys. Rev. B **74**, 195419 (2006).
[29] M. A. Romero, S. C. Gómez-Carrillo, P. G. Bolcatto, and E. C. Goldberg, J. Phys.: Condens. Matter **21**, 215602 (2009).
[30] F. Bonetto, M. A. Romero, Evelina A. García, R. A. Vidal, J. Ferrón, and E. C. Goldberg, Phys. Rev. B **78**, 075422 (2008).
[31] Evelina A. García, M. A. Romero, C. González, and E. C. Goldberg, Surf. Sci. **603**, 597 (2009).
[32] A. Jerez, P. Vitushinsky, and M. Lavagna, Phys. Rev. Lett. **95**, 127203 (2005).
[33] Y. Ji, M. Heiblum, D. Sprinzak, D. Mahalu, and H. Shtrikman, Science **290**, 779 (2000).
[34] U. Gerland, J. von Delft, T. A. Costi, and Yuval Oreg, Phys. Rev. Lett. **84**, 3710 (2000).
[35] Y. Ji, M. Heiblum, and H. Shtrikman, Phys. Rev. Lett. **88**, 076601 (2002).
[36] T. L. Einstein, Phys. Rev. B **11**, 577 (1975).
[37] A. Martín-Rodero, F. Flores, M. Baldo, and R. Pucci, Solid State Commun. **44**, 911 (1982).
[38] E. C. Goldberg and M. C. G. Passeggi, J. Phys.: Condens. Matter **8**, 7637 (1996).
[39] A. C. Hewson, *The Kondo Problem to Heavy Fermions* (Cambridge University Press, Cambridge, 1993).
[40] L. V. Keldysh, Zh. Eksp. Teor. Fiz. **47**, 1515 (1964) [Sov. Phys. JETP **20**, 1018 (1965)].
[41] J. A. Appelbaum and D. R. Penn, Phys. Rev. **188**, 874 (1969).
[42] J. A. Appelbaum and D. R. Penn, Phys. Rev. B **3**, 942 (1971).
[43] L. Dworin, Phys. Rev. **164**, 818 (1967); **164**, 841 (1967).
[44] A. Oguchi, Prog. Theor. Phys. **43**, 257 (1970).
[45] R. Schuster, E. Buks, M. Heiblum, D. Mahalu, V. Umansky, and H. Shtrikman, Nature (London) **385**, 417 (1997).